Current Biology *16*, 717–722, April 4, 2006 ©2006 Elsevier Ltd All rights reserved DOI 10.1016/j.cub.2006.02.068

Report

Nap1 Regulates *Dictyostelium* Cell Motility and Adhesion through SCAR-Dependent and -Independent Pathways

Neysi Ibarra,[1,3] Simone L. Blagg,[1,3] Francisca Vazquez,[2] and Robert H. Insall[1,*]
[1] School of Biosciences
University of Birmingham
Edgbaston
Birmingham B15 2TT
United Kingdom
[2] Department of Cell Biology
Johns Hopkins University
School of Medicine
725 N. Wolfe St., 114 WBSB
Baltimore, Maryland 21205

Summary

SCAR—also known as WAVE—is a key regulator of actin dynamics. Activation of SCAR enhances the nucleation of new actin filaments through the Arp2/3 complex, causing a localized increase in the rate of actin polymerization [1]. In vivo, SCAR is held in a large regulatory complex, which includes PIR121 and Nap1 proteins, whose precise role is unclear. It was initially thought to hold SCAR inactive until needed [2], but recent data suggest that it is essential for SCAR function [3]. Here, we show that disruption of the gene that encodes Nap1 (*nap*A) causes loss of SCAR function. Cells lacking Nap1 are small and rounded, with diminished actin polymerization and small pseudopods. Furthermore, several aspects of the *nap*A phenotype are more severe than those evoked by the absence of SCAR alone. In particular, *nap*A mutants have defects in cell-substrate adhesion and multicellular development. Despite these defects, *napA*$^-$ cells move and chemotax surprisingly effectively. Our results show that the members of the complex have unexpectedly diverse biological roles.

Results and Discussion

WASP is autoinhibited in its native state, and this inhibition may be relieved by binding of Cdc42 to the GBD (GTPase binding domain) of WASP [4]. SCAR, however, contains no GBD domain, and pure SCAR is active in the absence of activators [5]. In vivo, SCAR exists within a heteropentameric complex [2] consisting of Nap1, PIR121, Abi1 or 2, and HSPC300 [2]. By controlling the stability, localization, and function of SCAR, these proteins are thought to guarantee that Arp2/3 activation remains rigorously dependent on signals. Recent biochemical and genetic studies have provided contradictory evidence as to the nature and regulation of the SCAR complex in vivo [2, 3, 6–13]. Following our earlier consideration of *pir*A mutants, we identified the single *Dictyostelium* *nap*A gene, Dictybase reference DDB0167739, with a predicted size of 1160 amino acids. No other predicted proteins yielded significant alignments. Unusual for a protein of such size, the alignment between predicted human and *Dictyostelium* proteins runs continuously throughout the entire length of the proteins (Figure S1 in the Supplemental Data available online), with only short gaps and an overall 26% amino acid identity. More unusual still, for a conserved protein of this size, was the absence of any known protein homology domains as detected by either SMART or PFAM searches. As predicted from other organisms, the *Dictyostelium* Nap1 protein forms part of the SCAR complex. Expression of myc-tagged Nap1 in AX3 cells followed by western blotting yielded a band with the expected size of around 140 kDa; immunoprecipitation of endogenous PIR121 showed that NAP1 associates quantitatively with SCAR and PIR121 (Figure 1A). The reverse immunoprecipitation with anti-SCAR also quantitatively pulls down PIR121 (Figure 1B), confirming that *Dictyostelium* Nap1 and PIR121 are found in a single tight complex with SCAR in vivo.

Regulation of PIR121 and SCAR Levels In Vivo

SCAR and PIR121 levels are greatly decreased in cells where one SCAR-complex member has been removed either genetically [6] or by RNAi [7]. We therefore examined SCAR protein levels in *nap*A$^-$ mutants (Figure 1C). Like *pir*A null mutants, *nap*A$^-$ and *nap*A$^-$/*pir*A$^-$ mutants have very low levels (at least 10-fold reduced) of SCAR. The quantity of SCAR was, however, similar in all three mutants.

The loss of SCAR in different mutants of the regulatory complex has led to a presumption that loss of any member of the complex causes degradation of all the remaining complex members [3, 7, 12]. To test this idea, we examined the levels of PIR121 in our various mutants (Figure 1C). The protein is detectable in the absence of other complex members, although its level varies depending on the complex member disrupted. We found very little alteration in PIR121 in *scar* null cells, whereas *nap*A null and *napA*/*scar* double null mutants contain approximately half the wild-type level, a far less emphatic change than the near-total loss of SCAR. This suggests that the presence or absence of SCAR is not particularly important for the stability of the regulatory complex, whereas Nap1 protects PIR121 from degradation. This is in agreement with recent results showing that PIR121 and Nap1 form an independent complex together in vitro [14].

Nap1 Is Required for SCAR Function

We generated *napA* null mutants by homologous recombination in *Dictyostelium* strain AX3, then assayed cell shape, movement, and chemotaxis toward folate by using under-agar assays [15]. Wild-type cells extend a number of large pseudopods and move quickly toward the stimulus (Figure 2 and Movie 1). In contrast,

*Correspondence: r.h.insall@bham.ac.uk
[3] These authors contributed equally to this work.

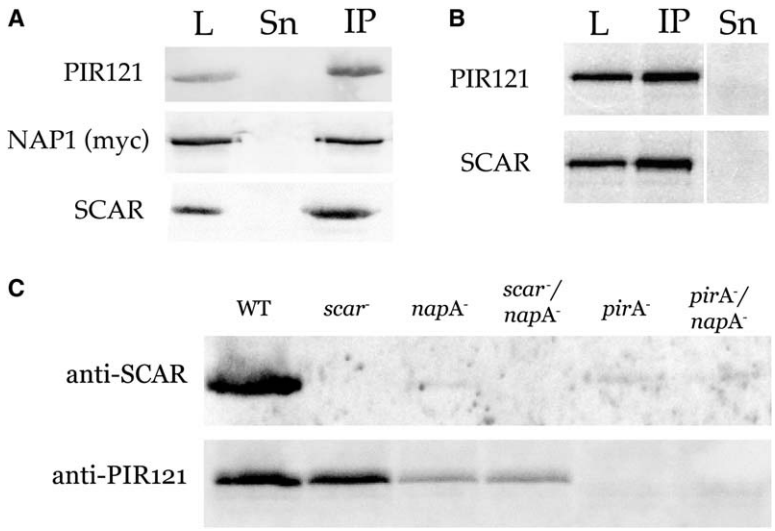

Figure 1. The *Dictyostelium* SCAR Complex

(A) Coimmunoprecipitation of members of the SCAR complex by anti-PIR121 antibodies. PIR121, SCAR, and myc-tagged Nap1 were all present in the lysate (L) but quantitatively removed from the supernatant (Sn) after immunoprecipitation. All three subunits were present in the immunoprecipitate (IP) brought down by using protein G agarose. Control lanes with no primary antibody did not contain PIR121, SCAR, or myc-NAP1.

(B) Reverse coimmunoprecipitation with anti-SCAR. PIR121 was present in the lysate and the immunoprecipitate but not the supernatant. Control lanes with no primary antibody did not contain PIR121 or SCAR.

(C) Changes in SCAR and PIR121 protein levels in mutant cells. Western blots showing SCAR protein (top panel) and PIR121 protein (bottom panel) in growing cells are displayed. Equal quantities of protein were western blotted and probed with anti-SCAR and ant-PIR antibodies. Full-length SCAR protein is clearly visible in wild-type (AX3) cells, but was almost undetectable in *nap*A$^-$, *pir*A$^-$, and *nap*A$^-$/*pir*A$^-$ mutants. PIR121 protein is normal in *scar*$^-$ mutants, whereas levels are reduced in *nap*A$^-$ and *nap*A$^-$/*scar*$^-$ mutants.

*nap*A$^-$ mutants move more slowly toward the chemoattractant, appear more rounded, and extend much smaller protrusions (Figure 2 and Movie 2). The *nap*A$^-$ cells are clearly smaller and less motile than the parent, with smaller actin structures and a large reduction in the levels of F-actin, even greater than that seen in *scar*$^-$ mutants (Figure 2; Table S1). To verify that these mutants act through the same pathway, we also generated *nap*A disruptions in a *scar*$^-$ background and compared wild-type, *nap*A$^-$, *scar*$^-$, and *nap*A$^-$/*scar*$^-$ cells (Figure 2, Movies 1–4). All these mutants are less motile, in contrast to *pir*A null cells, which, as we have previously shown [6], have an overactive SCAR phenotype (also Figure 2 and Movie 5).

Nap1 Is Required for the pir*A* Null Phenotype

In order to ascertain the interplay between complex members Nap1 and PIR121, we also generated a *nap*A$^-$/*pir*A$^-$ double mutant. We observed these mutant cells chemotaxing under agar and found that they extended extremely small pseudopods and moved very similarly to *nap*A null mutants (Figure 2A and Movie 6). This is in great contrast to *pir*A null cells, which extend very long pseudopods from multiple locations, indicative of overactive SCAR [6] (Figure 2A and Movie 5). As seen previously, *scar*$^-$/*pir*A$^-$ double mutants resemble single *scar*$^-$ mutants. In addition, resting *pir*A null cells have an extremely high F-actin content, whereas *nap*A/*pir*A double null mutants have the same F-actin content as *nap*A null cells (Figure 2B). This shows that Nap1 is required for the *pir*A null phenotype, presumably because it is required for constitutive SCAR activity.

Nap1 and SCAR Are Not Essential for Responses to Chemoattractants

Cells can still move and chemotax without SCAR and/or Nap1. Pseudopods in mutant cells are clearly initiated and protruded, although they are smaller than wild-type pseudopods. This leads to locomotion that is clearly different, but still efficiently controlled by chemotactic signals. This contrasts with reports from other cell types showing SCAR proteins are essential for the generation of actin pseudopods (for example, [3]).

When cells are stimulated with chemoattractants, the Arp2/3 complex briefly redistributes from the soluble cytosol to an insoluble fraction [16]. One would therefore expect a comparable increase in the amount of cytoskeleton-associated SCAR after chemoattractant stimulation. To test this prediction, we stimulated wild-type cells with cAMP and assessed different subcellular fractions for the presence of SCAR, PIR121, and the Arp2/3 complex. As Figure 3A shows, all relocate from the cytoplasm to the insoluble fraction within 10 s of chemoattractant stimulation. This is accompanied by an increase in the proportion of the cell edge with localized SCAR (Figure S2).

We then assayed F-actin levels in cAMP-stimulated Nap1- and SCAR-deficient strains [17, 18]. In wild-type cells, there is a rapid rise in F-actin content, peaking at approximately 4–6 s after addition of cAMP, followed by a smaller rise between 30–60 s. No major difference was found in the relative change of F-actin content in wild-type, *scar*$^-$, *nap*A$^-$, and *nap*A$^-$/*scar*$^-$ mutants following stimulation with cAMP (Figure 3B). All strains have a sharp initial peak within the first 10 s as observed in previous studies [19]. The initial rise in the F-actin content of *scar*$^-$, *nap*A$^-$, and *nap*A$^-$/*scar*$^-$ mutants appears to peak slightly later, with F-actin reaching its height at about 8–10 s after cAMP addition (Figure 3B).

These data together show that Nap1- and SCAR-deficient cells can still respond to chemoattractants and that at least some signaling pathways involved in F-actin polymerization in response to signals are intact. We therefore infer that the chemoattractant-dependent actin nucleation observed in Figure 3B is not exclusively regulated by SCAR and may not involve SCAR or its

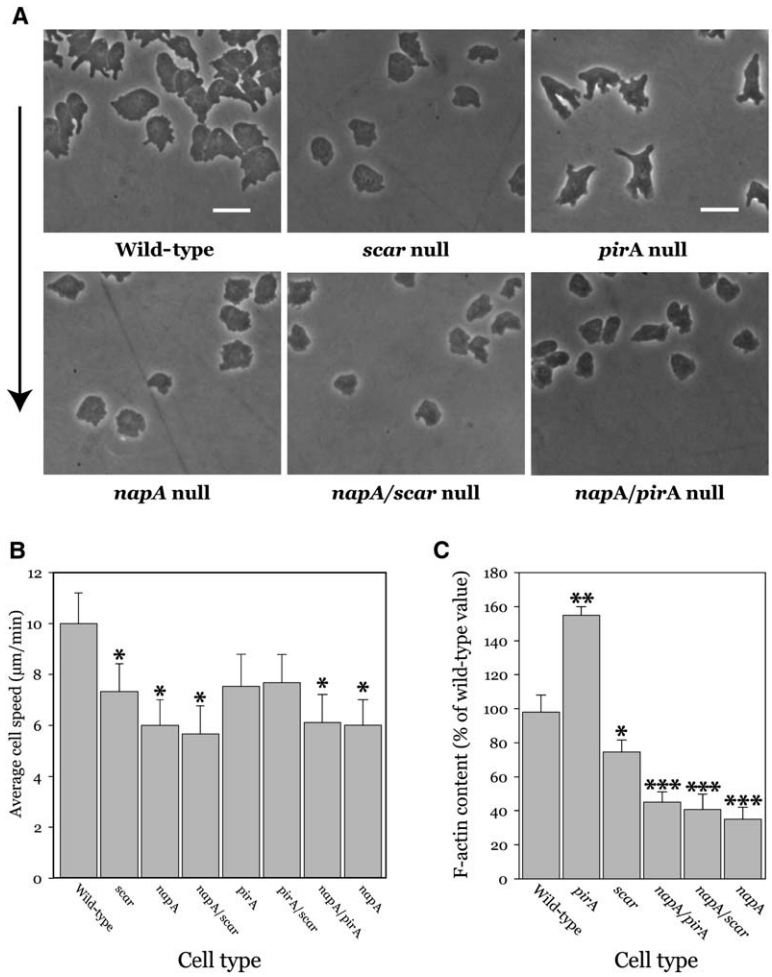

Figure 2. Cell Motility and Actin Defects in Mutants

(A) Under-agar chemotaxis assay. Cells moving up a folate gradient under a layer of agarose are shown by using phase contrast. The direction of chemotaxis is indicated by the arrow. The scale bar represents 25 μm.

(B) Mean cell speed of wild-type and mutant cells. Movies of chemotaxing cells were analyzed as described in [6]. Speeds were determined by calculating the distance moved by cell centroids in consecutive frames. Bars show standard deviations of means from several cells ($n \geq 6$).

(C) Resting F-actin content. The relative amounts of F-actin in unstimulated wild-type and mutant cells were determined by using a phalloidin binding assay. All results were normalized to the F-actin levels of unstimulated wild-type cells. Bars show standard deviations from multiple samples ($n \geq 3$) taken on the same day. Single asterisk indicates significantly less than wild-type ($p < 0.01$); double asterisk indicates significantly more than wild-type ($p < 0.01$); triple asterisk indicates significantly less than wild-type and also less than *scar* mutant ($p < 0.05$).

regulatory complex at all. Other Arp2/3 activators (for example, WASP [20]) as well as other actin nucleators (for example, formins, reviewed in [21]) may be responsible for the increase in actin polymerization upon cAMP stimulation.

Nap1 Has Additional Functions Independent of SCAR

We examined the phenotypes of *nap*A$^-$ mutants in other processes that use actin. First, we analyzed multicellular development. This involves multiple aspects of cell movement, adhesion, and contractility and has therefore been a useful signpost for phenotypes in mutants lacking, for example, actin binding proteins [22] or myosins [23]. The aggregation and development of *scar* and *pirA* mutants are, surprisingly, nearly normal. *nap*A null cells, however, show small but clear developmental phenotypes. Aggregation started later than in wild-type, and the aggregates that were formed were relatively small (Figure S3). The clearest phenotype was seen in phototaxis assays (Figure 4). Although *nap*A mutants were able to form normal (but relatively small) slugs, the ability of these slugs to perform phototaxis toward a directional light source was greatly diminished. We suspect that this phenotype is caused by mechanical weakness of the slugs, rather than a sensory defect; *nap*A mutant slugs seemed able to orient, but unable to break out of the main clump of cells in the assay. *scar*$^-$ mutants had no such problem (Figure 4).

A quantitative analysis of cell-substrate adhesion in vegetative cells revealed a serious defect in *nap*A$^-$ cells (Table S2). Mutants were far less resistant to moderate conditions of shear stress than the wild-type. Unexpectedly, this phenotype was far more severe in *nap*A$^-$ cells than in either *scar*$^-$ or *pir*A$^-$ mutants. By way of a comparison, we examined other lines with defects in cell-substrate adhesion. The *nap*A$^-$ cells adhered to substrate as poorly as well-known adhesion mutants such as talin and myosin VII (Table S2). Therefore Nap1, using a mechanism that works independently of SCAR and PIR121 function, appears to be required for adhesion to a substrate. Further evidence that cell-cell, as well as cell-substrate adhesion, was affected in *nap*A mutants came from examination of slug trails (Figure S3B). Mutant slugs appeared to lose cells from the rear, resulting in a trail that was studded with sloughed cells, and slugs that migrated any distance lost so much material that they were barely able to culminate. Again, none of these defects were observed in either *pir*A or *scar* mutants.

The more severe phenotypes seen in *nap*A mutants than in either *scar* or *pir*A mutants are intriguing. Disruption of the *nap*A gene resulted in a further decrease in F-actin content, smaller and less motile cells, and poor

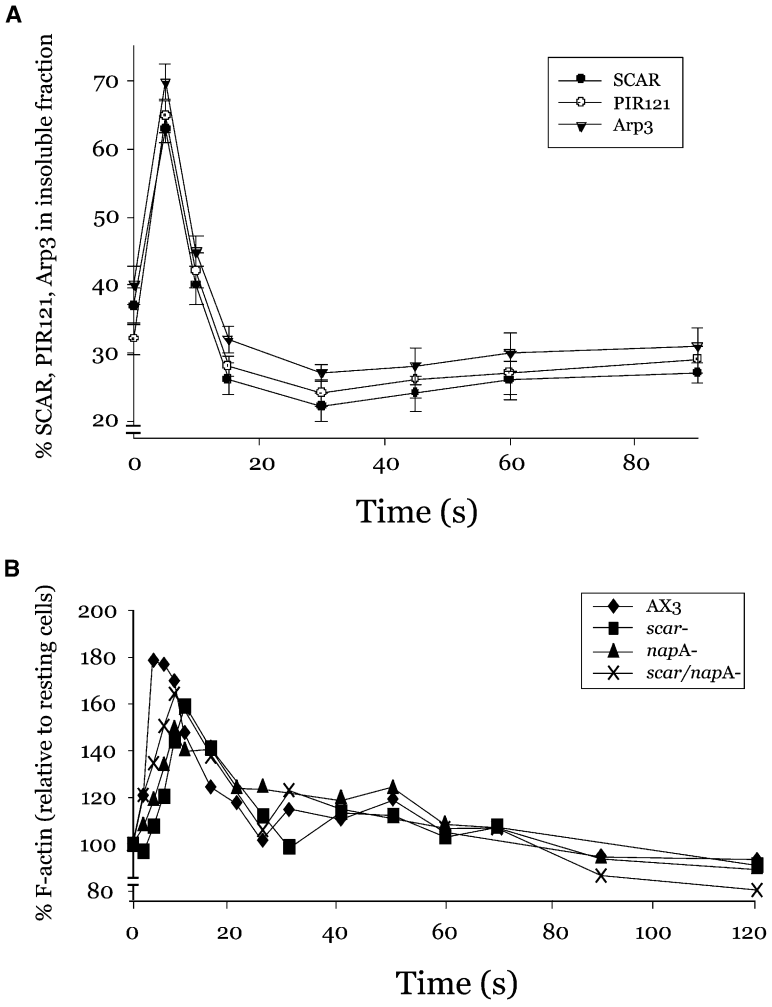

Figure 3. *scar* and *nap*A Mutants Can Respond to cAMP

(A) SCAR translocation upon cAMP stimulation. Aggregation-competent cells were stimulated with cAMP. At different times after stimulation, cells were filter-lysed and centrifuged. The pellets were separated by SDS-PAGE, blotted onto nitrocellulose, and probed with anti-PIR121, anti-Arp3, and anti-SCAR polyclonal antibodies and developed by using ECL. Band intensities were quantified by using ImageJ. The proportion of SCAR and PIR121 translocated to the cytoskeleton and membrane fraction increased in the same fashion as for the Arp2/3 complex [16]. Data are from three independent experiments performed in duplicate; bars show standard deviations.

(B) Changes in F-actin in response to chemoattractant. A phalloidin binding assay was used to measure changes in F-actin levels in wild-type and mutant cells in response to stimulation with 1 μM cAMP. Values are normalized as the percentage of the F-actin content of unstimulated cells for each mutant.

cell adhesion compared to *scar* null cells. Nap1 is clearly involved in several processes in the absence of SCAR (the phenotypes of *nap*A mutations are worse than those of *scar* mutations), whereas loss of SCAR does not seem to affect the severity of *nap*A mutations (*nap*A and *scar*/*nap*A mutants are similar in every process we have

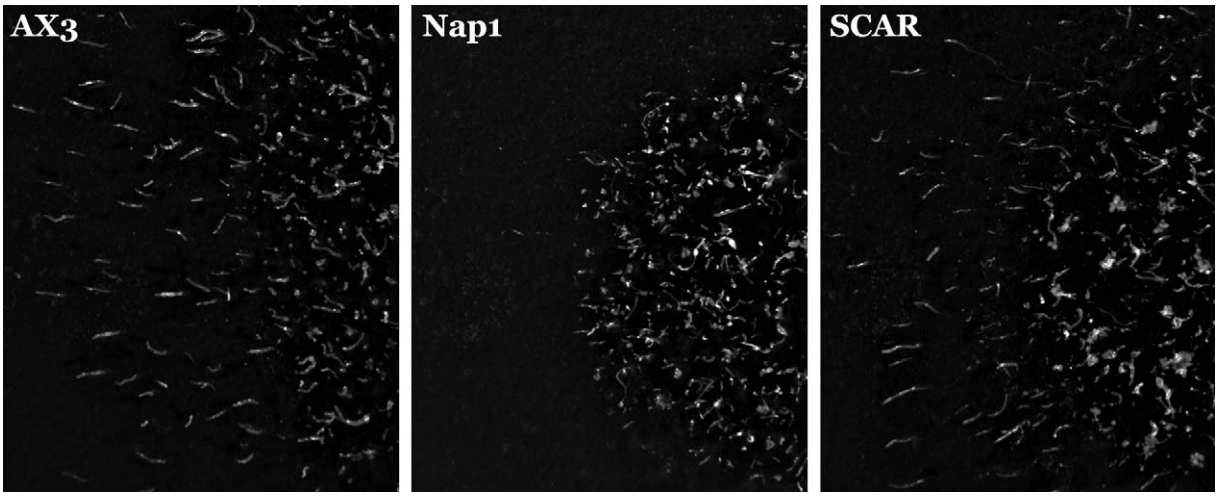

Figure 4. Failure of Phototaxis in *nap*A but Not *scar* Mutants

Cells were grown in axenic medium, and then 5×10^7 cells were washed in water and deposited onto wet black millipore filters and incubated for 3 days in the presence of a unidirectional light source. The resultant slugs and slug trails were photographed.

observed). This leads us to conclude that Nap1 is a component of one or more SCAR-independent pathways that regulate actin dynamics and cell adhesion, in addition to its well-known role as a SCAR regulator.

The results we present here suggest that different members of the complex have separable roles. It appears that Nap1 is essential for all SCAR activity, whereas PIR121 is required to hold SCAR in an inactive state. Our data are thus not consistent with either simple model of SCAR function. The loss of function in *nap*A$^-$ cells is not compatible with simple constitutive activity of uncomplexed SCAR, but the opposite roles of Nap1 and PIR121 do not agree with the complex acting as an undifferentiated, continuous unit. Recent examination of the Nap1 homolog in mammalian neutrophils suggests that this is indeed true [24]. Further analysis of unknown binding partners and targets of Nap1 will reveal which roles are SCAR-independent and which are part of the better-known SCAR pathway.

Experimental Procedures

Cell Culture and Development

Dictyostelium discoideum cells were grown axenically in HL-5 medium, at 22ºC either in Petri dishes or shaken in flasks. For experiments requiring bacterially grown cells, *Dictyostelium* were plated onto lawns of *Klebsiella aerogenes* and harvested after 48 hr by repeated washing in KK_2 buffer. For experiments requiring developed cells, *Dictyostelium* were harvested from *Klebsiella* lawns, starved for 1 hr by shaking in KK_2 buffer, and then treated with 0.1 μM cAMP every 6 min for 4 hr, while being slowly shaken at a density of 2×10^7 cells/ml.

Generation of Gene Disruptants

The *Dictyostelium* homologs of Nap1 and the other members of the complex were identified by BLAST searches against the libraries of the Tsukuba *Dictyostelium* cDNA project and the *Dictyostelium* genome project in Köln. A 1.4 kbp section of the 3′ end of the *nap*A gene was amplified from genomic DNA by PCR. The resulting fragment was then cloned into pBluescript, and subsequently a blasticidin resistance cassette was cloned into an EcoR1 site in the gene. This construct was electroporated into *Dictyostelium* AX3 cells, and subsequent blasticidin-resistant colonies were screened for gene disruption with PCR and Southern blotting. The tagged Nap1 was generated by adding an N-terminal myc-tag to a full-length cDNA by PCR and then expressing the construct under the control of an Act15 promoter in the extrachromosomal expression vector pJK1.

The double *nap*A/*scar* null mutant was generated with the *nap*A construct described above, with *scar*$^-$ cells [6] as the parental strain.

The double *nap*A/*pir*A null mutant was generated with the *pir*A construct [6], with *nap*A$^-$ cells as the parental strain.

Under-Agar Chemotaxis Assays

We used the previously described method for imaging *Dictyostelium* cells moving toward a folate stimulus under a thin layer of agarose [15]. Cells were imaged moving under the agar toward the folate stimulus by using phase-contrast microscopy over the next 6–8 hr. To measure cell speeds, we used an NIH image macro to calculate the mean displacement of cell centroids, sampling frames 30 s apart.

Actin-Polymerization Assays

To determine changes in F-actin over time in response to 1μM cAMP stimulation, we used a phalloidin-based assay as previously described [17, 18]. In brief, 100 μl aliquots of developed cells at 2×10^7 cells/ml were incubated with 1 μM of cAMP for a set period of time before fixing by addition of 0.9 ml stop solution (3.7% formaldehyde, 0.1% Triton X-100, 0.5mM TRITC-phalloidin in G buffer, 20 mM KPO_4, 10 mM PIPES, 5 mM EGTA, 2 mM $MgCl_2$, pH 6.8). Zero time points (no stimulus added) were performed in triplicate. Samples were then incubated with mixing for 1 hr before centrifuging at full speed and washing in G buffer with 0.1% saponin for 1 hr. Samples were then recentrifuged, and 1.4 ml methanol was added to each pellet. After incubation, the samples were then centrifuged and the fluorescence of the supernatant was measured in a spectrofluorimeter. For the determination of resting F-actin content, cells were harvested from bacteria and resuspended at a density of 2×10^7/ml and assayed as described above, without adding stimulus.

Generation of PIR121 and SCAR Antibodies

For the production of the PIR121 and SCAR antigens, fragments of PIR121 and SCAR were cloned into the expression vector pMW172 expressed in *E. coli* strain BL21, and inclusion bodies were induced, purified, and prepared according to [22]. PIR121 and SCAR fragments were isolated and injected into sheep and rabbit, respectively. When necessary, anti-PIR121 and anti-SCAR antibodies were affinity purified.

Immunoprecipitation

Axenically grown *Dictyostelium* cells were washed and resupended in ice-cold lysis buffer (200 mM sucrose, 10 mM Tris, 1 mM EDTA, 50 mM KCl, 1 mM DTT, 100 μM AEBSF, 0.2 μM TLCK, pH 7.5). The suspension was filtered in a filter unit by using a 5 μm TMTP membrane filter (Millipore) and centrifuged (1 min, full-speed, Eppendorf microfuge). Cleared lysates were incubated with protein G-Sepharose beads coupled to affinity-purified anti-PIR121 polyclonal antibody for 2 hr at 4ºC. Precipitates were resolved by SDS-PAGE and analyzed by immunoblotting. Full-length Nap1 was myc-tagged and cloned in an extrachromosomal vector for exogenous expression in AX3 cells.

SCAR Translocation

Developed cells were resupended in KK2 buffer and stimulated with 10 μM cAMP. At specific time points, samples were resuspended in lysis buffer (200 mM sucrose, 10 mM Tris, 1 mM EDTA, 50 mM KCl, 1 mM DTT, 100 μM AEBSF, 0.2 μM TLCK, pH 7.5) and filtered through a 5 μm TMTP membrane filter (Millipore). Samples were centrifuged for 1 min at full speed, and the pellet was solubilized in SDS sample buffer. The samples were resolved by SDS-PAGE and analyzed by immunoblotting.

Development

Cells grown in axenic medium were washed twice in 10 mM Na/K phosphate buffer and allowed to develop on nitrocellulose filters. For the slug migration assay (phototaxis assay), cells were plated on nonnutrient agar plates and allowed to migrate on water agar for 24 hr toward a unidirectional light source.

Supplemental Data

Supplemental Data include Supplemental Experimental Procedures, three figures, and two tables and are available with this article online at: http://www.current-biology.com/cgi/content/full/16/7/717/DC1/.

Acknowledgments

R.H.I. is supported by a Medical Research Council (MRC) senior fellowship, S.L.B is supported by a Biotechnology and Biological Sciences Research Council (BBSRC) postgraduate studentship, and N.I is supported by The Darwin Trust of Edinburgh postgraduate studentship. This work was also supported by a project grant from the BBSRC (G17939). We are grateful to Alice Pollitt for help with data interpretation, to Laura Machesky, Mehreen Zaki, and Alice Pollitt for helpful discussions and comments on the text, and to the constant assistance of the Japanese cDNA projects for clones and information.

Received: February 7, 2005
Revised: February 14, 2006
Accepted: February 17, 2006
Published: April 3, 2006

References

1. Pollard, T.D., Blanchoin, L., and Mullins, R.D. (2000). Molecular mechanisms controlling actin filament dynamics in nonmuscle cells. Annu. Rev. Biophys. Biomol. Struct. *29*, 545–576.
2. Eden, S., Rohatgi, R., Podtelejnikov, A.V., Mann, M., and Kirschner, M.W. (2002). Mechanism of regulation of WAVE1-induced actin nucleation by Rac1 and Nck. Nature *418*, 790–793.
3. Steffen, A., Rottner, K., Ehinger, J., Innocenti, M., Scita, G., Wehland, J., and Stradal, T.E. (2004). Sra-1 and Nap1 link Rac to actin assembly driving lamellipodia formation. EMBO J. *23*, 749–759.
4. Kim, A.S., Kakalis, L.T., Abdul-Manan, N., Liu, G.A., and Rosen, M.K. (2000). Autoinhibition and activation mechanisms of the Wiskott-Aldrich syndrome protein. Nature *404*, 151–158.
5. Machesky, L.M., and Insall, R.H. (1998). Scar1 and the related Wiskott-Aldrich syndrome protein, WASP, regulate the actin cytoskeleton through the Arp2/3 complex. Curr. Biol. *8*, 1347–1356.
6. Blagg, S.L., Stewart, M., Sambles, C., and Insall, R.H. (2003). PIR121 regulates pseudopod dynamics and SCAR activity in Dictyostelium. Curr. Biol. *13*, 1480–1487.
7. Kunda, P., Craig, G., Dominguez, V., and Baum, B. (2003). Abi, Sra1, and Kette control the stability and localization of SCAR/WAVE to regulate the formation of actin-based protrusions. Curr. Biol. *13*, 1867–1875.
8. Rogers, S.L., Wiedemann, U., Stuurman, N., and Vale, R.D. (2003). Molecular requirements for actin-based lamella formation in Drosophila S2 cells. J. Cell Biol. *162*, 1079–1088.
9. Basu, D., El-Assal, S.-D., Le, J., Mallery, E.L., and Szymanski, D.B. (2004). Interchangeable functions of Arabidopsis PIROGI and the human WAVE complex subunit SRA1 during leaf epidermal development. Development *131*, 4345–4355.
10. Deeks, M.J., Kaloriti, D., Davies, B., Malho, R., and Hussey, P.J. (2004). Arabidopsis NAP1 is essential for Arp2/3-dependent trichome morphogenesis. Curr. Biol. *14*, 1410–1414.
11. El-Assal, S.-D., Le, J., Basu, D., Mallery, E.L., and Szymanski, D.B. (2004). Arabidopsis GNARLED encodes a NAP125 homolog that positively regulates ARP2/3. Curr. Biol. *14*, 1405–1409.
12. Innocenti, M., Zucconi, A., Disanza, A., Frittoli, E., Areces, L.B., Steffen, A., Stradal, T.E., Di Fiore, P.P., Carlier, M.F., and Scita, G. (2004). Abi1 is essential for the formation and activation of a WAVE2 signalling complex. Nat. Cell Biol. *6*, 319–327.
13. Blagg, S.L., and Insall, R.H. (2004). Control of SCAR activity in Dictyostelium discoideum. Biochem. Soc. Trans. *32*, 1113–1114.
14. Gautreau, A., Ho, H.Y., Li, J., Steen, H., Gygi, S.P., and Kirschner, M.W. (2004). Purification and architecture of the ubiquitous Wave complex. Proc. Natl. Acad. Sci. USA *101*, 4379–4383.
15. Laevsky, G., and Knecht, D.A. (2001). Under-agarose folate chemotaxis of Dictyostelium discoideum amoebae in permissive and mechanically inhibited conditions. Biotechniques *31*, 1140–1149.
16. Insall, R., Muller-Taubenberger, A., Machesky, L., Kohler, J., Simmeth, E., Atkinson, S.J., Weber, I., and Gerisch, G. (2001). Dynamics of the Dictyostelium Arp2/3 complex in endocytosis, cytokinesis, and chemotaxis. Cell Motil. Cytoskeleton *50*, 115–128.
17. Peracino, B., Borleis, J., Jin, T., Westphal, M., Schwartz, J.M., Wu, L.J., Bracco, E., Gerisch, G., Devreotes, P., and Bozzaro, S. (1998). G protein beta subunit-null mutants are impaired in phagocytosis and chemotaxis due to inappropriate regulation of the actin cytoskeleton. J. Cell Biol. *141*, 1529–1537.
18. Hall, A.L., Schlein, A., and Condeelis, J. (1988). Relationship of pseudopod extension to chemotactic hormone-induced actin polymerization in amoeboid cells. J. Cell. Biochem. *37*, 285–299.
19. Hall, A.L., Warren, V., Dharmawardhane, S., and Condeelis, J. (1989). Identification of actin nucleation activity and polymerization inhibitor in ameboid cells: Their regulation by chemotactic stimulation. J. Cell Biol. *109*, 2207–2213.
20. Derry, J.M., Ochs, H.D., and Francke, U. (1994). Isolation of a novel gene mutated in Wiskott-Aldrich syndrome. Cell *79*, 922.
21. Zigmond, S. (2004). Formin-induced nucleation of actin filaments. Curr. Opin. Cell Biol. *16*, 99–105.
22. Kelleher, J.F., Atkinson, S.J., and Pollard, T.D. (1995). Sequences, structural models, and cellular localization of the actin-related proteins Arp2 and Arp3 from Acanthamoeba. J. Cell Biol. *131*, 385–397.
23. De Lozanne, A., and Spudich, J.A. (1987). Disruption of the Dictyostelium myosin heavy chain gene by homologous recombination. Science *236*, 1086–1091.
24. Weiner, O.D., Rentel, M.C., Ott, A., Brown, G.E., Jedrychowski, M., Yaffe, M.B., Gygi, S.P., Cantley, L.C., Bourne, H.R., and Kirschner, M.W. (2006). Hem-1 complexes are essential for Rac activation, actin polymerization, and myosin regulation during neutrophil chemotaxis. PLoS Biol. *4*, e38.